energies

MDPI

Article

Endogenous Approach of a Frequency-Constrained Unit Commitment in Islanded Microgrid Systems

David Rebollal [1], Mónica Chinchilla [1], David Santos-Martín [1] and Josep M. Guerrero [2,*]

[1] Department of Electrical Engineering, University Carlos III of Madrid (UC3M), Avda. De la Universidad 30, Leganés, 28911 Madrid, Spain; drebolla@ing.uc3m.es (D.R.); mchin@ing.uc3m.es (M.C.); dsmartin@ing.uc3m.es (D.S.-M.)

[2] Center for Research on Microgrids (CROM), AAU Energy, Aalborg University, 9220 Aalborg East, Denmark

* Correspondence: joz@energy.aau.dk; Tel.: +45-2037-8262; Fax: +45-9815-1411

Abstract: Power reserves are usually scheduled in day-ahead unit commitment (UC) to minimize operating costs while maintaining system security. In applying basic UC (bUC) after a contingency, the system frequency may fall upon the activation of the load-shedding global control (under-frequency load-shedding or UFLS) limits. Small isolated microgrids are more sensitive to this issue due to their lack of inertia. Including dynamic considerations into the bUC problem can minimize UFLS activation and also avoid the need for the operator to later check the short-term feasibility of a bUC solution. These proposals are known as Frequency-Constrained UC (FCUC), although the implementation are very time-consuming. FCUC implementation will increase the system's operational costs, which should be calculated to estimate remuneration to the safety service based on the additional reserve provision. The electrical system of Gran Canaria island has suffered several episodes of greater blackouts in recent years. Shortly, there will be 242 MW of wind generation installed (26% of the thermal power installed on Gran Canaria). The main objective of this work is to improve the island system reliability by means of an FCUC formulation applied by the system operator in practice, including renewable sources. The results show that the frequency values remained within the admissible boundaries, but the system's operational costs increased by around 13%.

Keywords: frequency-constrained unit commitment; operating costs; reserve allocation; inertia; islanded microgrids

Citation: Rebollal, D.; Chinchilla, M.; Santos-Martín, D.; Guerrero, J.M. Endogenous Approach of a Frequency-Constrained Unit Commitment in Islanded Microgrid Systems. *Energies* **2021**, *14*, 6290. https://doi.org/10.3390/en14196290

Academic Editor: Gianfranco Chicco

Received: 22 July 2021
Accepted: 21 September 2021
Published: 2 October 2021

1. Introduction

Unit commitment (UC) tackles the problem of operating a system while optimizing its costs. To feed the load at any time, the UC algorithm decides, typically on an hourly basis, which generators must be online with their output power levels. The proposed cost-effective solution is analyzed in a further step to test the dynamic stability in the case of a contingency, for example, the sudden loss of the biggest online generator (N-1 criterion) [1]. If this exogenous evaluation rejects the proposal, the prior UC solution returns back to be reassessed until a new found UC solution is proven to be safe.

Although including dynamic considerations into the UC problem may be more time consuming, it can avoid the operator's need to later check the short-term feasibility of the UC solution. This is conducted endogenously by taking the dynamic risk within the constraints of the UC optimization problem into account.

During normal system operation, the frequency should be retained between certain thresholds around the nominal frequency. When a generating unit is suddenly disconnected, there is a power imbalance between generation and demand that causes a drop in the system frequency.

In the initial moments, the machines that are electrically closest to the event will nearly instantly supply the energy stored in the magnetic field [2]. Following the proximity effect, the natural response of synchronous units retains the frequency fall by providing the kinetic

energy of their rotating masses (inertia). The initial slope of the frequency fall, the rate of change of frequency (RoCoF), is given by the power imbalance size and the system inertia. For a given power imbalance, the more system inertia, the lower the frequency slope.

Thenceforth, the local droop-control of the generating units detects the variation in frequency and increases the power-regulator set point [3]. This safety mechanism is known as the primary regulation system response or primary frequency response (PFR). If the PFR is performed quickly enough, the generating power increases until both a new power balance and frequency nadir are reached, preventing the frequency from falling below a certain safety threshold. However, if it is not fast enough, the under-frequency relays would trip, activating the load-shedding global control, also known as under-frequency load shedding (UFLS) [4]. In the case of a lost generator, UFLS is an unwanted phenomenon that is more likely to occur in systems where synchronous generation units have been replaced by converter-based units that do not provide inertia and can also reduce the PFR [5].

Furthermore, small isolated microgrids are more sensitive to this issue due to their reduced inertia along with the bigger size of their generating units with respect to the system size. In large-scale power systems, if a sufficient reserve amount has been previously specified to establish energy equilibrium in the post-contingency steady state, then sufficient kinetic energy is stored in synchronous machines to avoid UFLS. However, in small power systems, such as microgrids on islands, with a significant proportion of variable generation connected through electronic converters, this criterion may be insufficient because an UFLS can occur in the transient frequency.

Frequency stability is considered one of the most relevant issues in the operation of isolated power systems [6]. An example showing the increasing RoCoF of a microgrid power system when the percentage-installed capacity of variable generation connected through power electronics increases is shown in [7]. UC procedures should consider these factors to ensure a reliable power supply while minimizing fuel costs. Therefore, UC optimization that considers the dynamic behaviour of the system seeks to ensure stable frequency operation by avoiding UFLS activation as a consequence of a loss of committed units.

General solutions to implement a UC that takes into account the limitations imposed by the frequency can be classified into four large groups: (1) including constraints to primarily limit the steady-state frequency [8], (2) coupling the reserve requirements and system dynamics using load–frequency sensitivity indexes [9], (3) including a mixed UC and grid simulation [10], and (4) controlling the minimum frequency of the power system [11]. In the case of microgrids on islands, the most effective method is to add dynamic constraints to the UC formulation (to guarantee the dynamic stability of these low-inertia systems) [12] and obtain an optimal solution, thus avoiding subsequent checks of the system dynamics, which are very costly in computing time. When dynamic constraints are included in the steady state UC (hereinafter referred to as basic UC or bUC), a family of modified optimization models is obtained, known in the literature as frequency-constrained UC (FCUC) or, in some cases, security-constrained UC (SCUC). There are mainly two ways to implement an FCUC. The first is through a very simplified version of the system's differential equations that govern the frequency decay after a contingency [13]. The work of [14] can be consulted for a detailed description of different approaches and comprehensive testing. Other works have considered frequency constraints in stochastic programming problems. Authors, such as [15], proposed two dynamic frequency constraints: one for the maximum RoCoF and a second for the minimum frequency (nadir) but using a very simplified model of the system. The second main way to implement an FCUC is with a more precise focus, as in [16] or [17]. Ref. [16] improves existing solutions (by means of including security constraints either indirectly or empirically defined) with respect to limiting the risk of UFLS. While the master problem handles the UC binary variables, the rest of the models are solved using a scheme similar to Bender's [14] in that they make use of Lagrange relaxation [18]. The drawback of the method is the long implementation time required by the optimizer.

The FCUC method proposed by [17] is applied to a two-area power system, significantly improving the frequency security of the system. It implies a minor increase (<1%) in the operational cost, although the assumptions made are theoretically hard to verify. The calculation times associated with these methods are relatively high, so in practice, they cannot be implemented in many of the procedures followed by the operators, who usually perform an hourly UC.

Table 1 summarizes the existing authors and methods of FCUC implementation, along with their disadvantages. A review of the state-of-the-art methods in the matter can be read in the study of [19]. The variability of the wind and photovoltaic resources and consequently of the generation of renewable sources is a subject widely studied in the literature that should also be taken into account in the FCUC formulation [20–22]. In recent years, different transmission system operators (TSO) have recognized the need for a sub-hourly programming timeframe (for example, 15 min) to better adapt to the variability introduced by renewable energy resources (RES) [23]. To the authors' knowledge, there is no adequate procedure that analyzes and, in practice, solves the problem of an FCUC applied to microgrids on islands with a growing increase in renewable generation.

Table 1. Ways to account for frequency in UC and associated authors.

Adding Indirect Constraints		**Post-Contingency Frequency Behavior Model**		**Directly Accounting for Frequency-Related Constraints in UC Models**	
Authors	**Disadvantage**	**Authors**	**Disadvantage**	**Authors**	**Disadvantage**
Restrepo (2005) [8]	More demanding computionally scheduling	Aik (2006) [24]	No guarantee of the dynamic stability of low-inertia systems	Teng (2016) [13]	Dynamics of the system are oversimplified
Ela (2012) [25]	Dynamics of the system are oversimplified and linearized	Ahmadi (2013) [26]	No guarantee of the dynamic stability of low-inertia systems	Cardozo (2018) [16]	Assumptions theoretically hard to verify
Ahmadi (2014) [27]	Cannot ensure satisfaction of the original constraint	Kerci (2019) [10]	No guarantee of the dynamic stability of low-inertia systems	Rabbanifar (2020) [17]	Theoretically hard to verify
Riaz (2019) [28]	Dynamics of the system are oversimplified and linearized	-	-	-	-

The case study in which the proposal of this article was tested is the isolated electrical system of Gran Canaria island, in the Canary Islands, Spain. Gran Canaria has 906 MW of installed capacity in two conventional thermal power plants, Barranco de Tirajana and Jinámar, in which there are diesel generators, gas/steam turbines, and combined cycles.

In 2020, Spain approved aids in EOLCAN [29] and SOLCAN [30] calls as well as European funds with which it is expected to increase the installed wind and photovoltaic power by 160 MW and 150 MW, respectively, throughout the archipelago. In June 2022, there will be 242 MW of wind generation installed on the island of Gran Canaria (there were 180 MW at the end of 2020) [31] with a consequent increase in variability, system inertia reduction, and an increase in the risk of unwanted frequency events. If there are no elements capable of countering this variation, the system security could be at risk.

The main contribution of this work is presenting a UC that is capable of avoiding the need for subsequent verification by including dynamic constraints and finding an optimal, direct, and safe solution in a reasonable amount of time. This optimal–safe solution is achieved and validated in the scheduling of island generators while paying attention to the increase in operating costs.

2. UC and Dynamic Models

2.1. UC with Exogenous Frequency Constraints, bUC Formulation

The objective of the UC problem is to minimize the total generating cost of the power system while satisfying constraints in regard to the expected energy demand, specific reserve requirements, and generator capabilities and availability. Frequently, a time horizon of seven days (168 h) or one day (24 h) is adopted when programming the power system operation, typically on an hourly basis. In this paper, in addition to RES, thermal units powered by fossil fuels, whose operating dynamics are relatively complex, are considered. For instance, the startup time required for a steam unit and its associated startup costs must be taken into account. Therefore, the formulation of the bUC problem requires the minimization of two cost terms. The first term is related to the energy produced and depends directly on the amount of fuel consumed; the second term reflects the start-up costs that vary with the boiler's temperature [32].

Scheduled units must also provide a reserve headroom to accommodate fluctuations in load or to cover equipment failures in emergency situations. Spinning reserve is the term used to describe the headroom capacity of the connected units. The amount of spinning reserve or capacity must comply with certain rules at all times, which are generally set by the bodies responsible for system reliability. Each hour, for instance, 5% of the spinning reserve might be required in excess of the expected system demand.

A thermal generating unit should not frequently switch between connected and disconnected modes due to the stress-damaging effects and the unit's own response time; in other words, once a thermal unit is shut down, it must remain disconnected for a minimum period, known as the minimum down-time, before it can be connected again. Similarly, once a thermal unit is started, it is required to remain connected for a minimum period, known as the minimum up-time, before it can be stopped again.

Another set of constraints that limits the ability of units to vary among scheduled levels of operation in short periods of time are their ramp constraints. When subject to ramp constraints, the units' generation levels are interdependent among all hours.

The bUC problem is formulated as a mixed integer programming problem. The mathematical formulation of the bUC problem is presented concisely below.

- Minimizing total generating costs:

$$\min_{\underline{u},\underline{x},\underline{p}} \sum_{t=1}^{T} \sum_{i=1}^{I} [C_i(p_{it}u_{it} + B_i(x_{i,t-1}, u_{it}, u_{i,t-1})] \quad (1)$$

where

i is the index for the number of units ($i = 1, \ldots, I$);
t is the index for time or nb of hours ($t = 0, \ldots, T$);
u_{it} is a binary variable defining if the unit i is committed or not at time t;
p_{it} is the power generated by unit i at time t;
C_i is the fuel cost of unit i at power i at time t;
B_i is the start-up cost;
x_i is the state variable denoting the time lenth a unit has been up or down.

- Demand constraint (load balancing equations):

$$\sum_{i=1}^{I} p_{it}u_{it} = D_t, t = 1, \ldots, T. \quad (2)$$

where D_t is the forecasted demand at period t.

- Spinning capacity constraint:

$$\sum_{i=1}^{I} p_i^{max} u_{it} \geq R_t, t = 1, \ldots, T, \tag{3}$$

where R_t is the spinning capacity requirement at period t.

- Ramp constraint:

$$p_{it} u_{it} - p_{i,t-1} u_{i,t-1} \geq \Delta_i(u_{i,t-1}, x_{it}), t = 1, \ldots, T; i = 1, \ldots, I, \tag{4}$$

where Δ_i is the generation level difference of unit i on any pair of consecutive on-line periods.

- Unit capacity constraint:

$$p_i^{min} \leq p_{it} \leq p_i^{max}, i = 1, \ldots, I; t = 1, \ldots, T. \tag{5}$$

- Commitment integer variables:

$$u_i t \in \{0, 1\}, i = 1, \ldots, I; t = 1, \ldots, T. \tag{6}$$

- Minimum up-time and down-time constraints:

$$x_{it} = \begin{cases} 1, if\ 1 \leq xit < t_i^{on} \\ 0, if\ -1 \geq x_{it} > -t_i^{off}, \\ 0\ or\ 1\ otherwise \end{cases} \tag{7}$$

- Initial conditions:

$$u_{i0} = \overline{u}_{i0},\ p_{i0} = \overline{p}_{i0},\ x_{i0} = \overline{x}_{i0},\ i = 1, \ldots, I. \tag{8}$$

Finally, the UC has to determine which generating units should be used at what hours to satisfy all the requirements at a minimum operating cost, assigning to each unit the power to be delivered at each moment. The basic UC flowchart can be seen in Figure 1. Some authors have incorporated a frequency-secured optimization framework for the procurement of an inertia [33] and frequency response [34], which enables the application of a marginal pricing scheme for these services.

In summary, bUC is a mixed integer optimization problem, in which it is difficult to obtain an optimal solution. For this purpose, the electrical system operator of the Canary Islands uses a proprietary tool, which contains the bUC problem constraints aforementioned in this section. Given that the tool used by the system operator currently does not incorporate frequency stability constraints, such as RoCoF or dynamic reserve, a bUC tool has been developed ad hoc in the Python programming language. This tool has been tested against the system operator tool with the purpose of validating it.

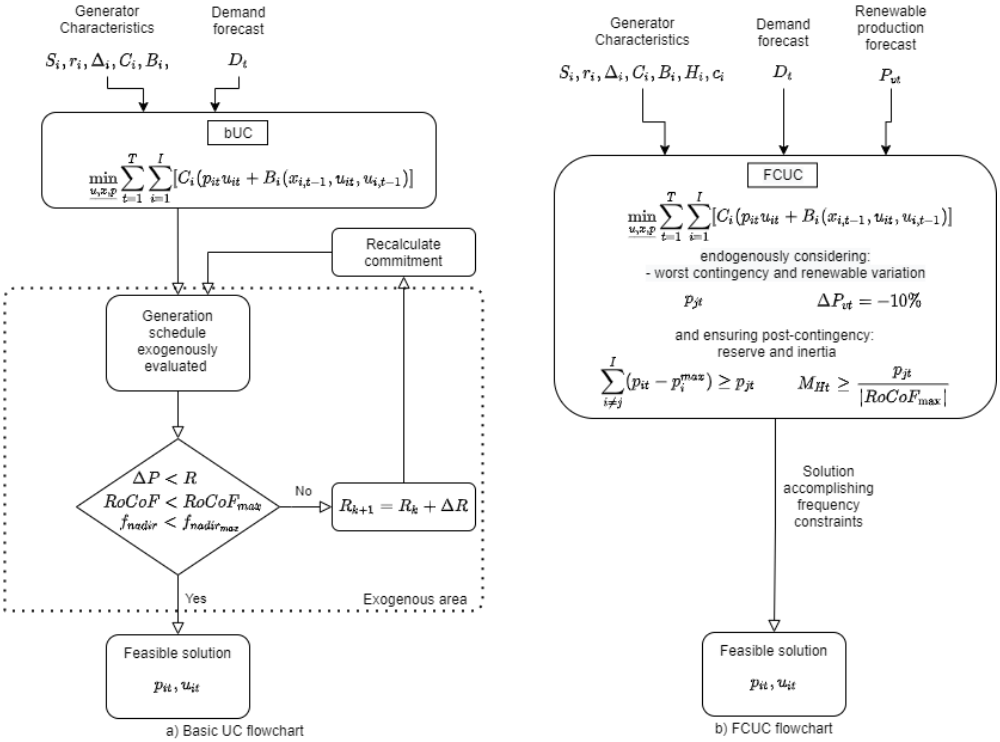

Figure 1. (**a**) bUC flowchart; (**b**) FCUC flowchart.

2.2. Frequency Response of Power Sources

The relationship between the generator power output change at a present time and the frequency is obtained from the basic expression of the dynamics of the system [35], where J is the system moment of inertia in kg·m^2, T_{net} is the net torque in N·m, and α and ω are the angular acceleration in rad/s^2 and speed in rad/s, respectively:

$$T_{net} = J\alpha = J\frac{d}{dt}\Delta\omega \tag{9}$$

and

$$\omega = \omega_0 + \alpha\Delta t \tag{10}$$

where t is the time in s.

The net power can be expressed as

$$P_{net} = P_m - P_e \tag{11}$$

where P_E is the prime mover power in W, and P_M is the electrical power in W. The zero subscript means the variable value at zero time, i.e., the initial condition.

$$P_m = P_{m0} - \Delta P_m \tag{12}$$

$$P_e = P_{e0} - \Delta P_e \tag{13}$$

Considering Equations (12) and (13) in Equation (11)

$$P_{net} = (P_{m0} - P_{e0}) + (\Delta P_m - \Delta P_e) \tag{14}$$

For torque:

$$T_{net} = T_m - T_e = (T_{m0} - T_{e0}) + (\Delta T_m - \Delta T_e) \tag{15}$$

where T_E is the prime mover torque in N·m and T_M the electrical torque in N·m.

$$P_{net} = \omega T_{net} \tag{16}$$

Equation (16) can be rewritten considering Equation (10):

$$P_{net} = (\omega_0 + \Delta\omega)T_{net} \tag{17}$$

Considering Equations (14) and (15) in Equation (17)

$$(P_{m0} - P_{e0}) + (\Delta P_m - \Delta P_e) = (\omega_0 + \Delta\omega)(T_{m0} - T_{e0}) + (\Delta T_m - \Delta T_e) \tag{18}$$

Assuming the balance in t_0:

$$P_{m0} = P_{e0} \tag{19}$$

$$T_{m0} = T_{e0} \tag{20}$$

Considering Equations (19) and (20) in Equation (18)

$$(\Delta P_m - \Delta P_e) = (\omega_0 + \Delta\omega)(\Delta T_m - \Delta T_e) \tag{21}$$

Neglecting the second-order terms ($\Delta\omega$ multiplying to ΔT),

$$(\Delta P_m - \Delta P_e) = \omega_0(\Delta T_m - \Delta T_e) \tag{22}$$

Thus, Equation (22) can be rewritten taking Equation (9) into account:

$$\Delta P_m - \Delta P_e = \omega_0 \, J \frac{d}{dt}\Delta\omega \tag{23}$$

The inertia constant H, in s, is defined as

$$H = \frac{\frac{1}{2}J\omega_0^2}{S_B} \tag{24}$$

where S_B is the base power in V·A, and consequently, the moment of inertia of the system, J, can be expressed as:

$$J = \frac{2HS_B}{\omega_0^2} \tag{25}$$

Taking Equation (25) in Equation (23):

$$\omega_0 \frac{2HS_B}{\omega_0^2} \frac{d}{dt}\Delta\omega = \Delta P_m - \Delta P_e \tag{26}$$

$$\frac{1}{\omega_0} \frac{d}{dt}\Delta\omega = \frac{1}{2H} \frac{\Delta P_m - \Delta P_e}{S_B} \tag{27}$$

Converting the mechanical speed of the shaft to frequency *(f)*, in Hz, through the relationship with the pairs of poles *(p)* $f = \frac{p}{2}\omega$ in Equation (27):

$$\frac{1}{f_0} \frac{d}{dt}\Delta f = \frac{1}{2H} \frac{\Delta P_m - \Delta P_e}{S_B} \tag{28}$$

It is usually expressed $2H$ as M_H:

$$\frac{1}{f_0} \frac{d}{dt}\Delta f = \frac{1}{M_H} \frac{\Delta P_m - \Delta P_e}{S_B} \tag{29}$$

Finally, expressing Equation (29) in values per unit for both Δf and ΔP results in

$$\frac{d}{dt}\Delta f = \frac{1}{M_H}\Delta P_m - \Delta P_e \tag{30}$$

which is known as the swing equation.

Dynamic Models

Once a solution to the bUC problem is found, the post-contingency system frequency must be checked afterwards to guarantee the system security in case an unwanted event occurs. For this purpose, software tools modeling the generator's physical parameters and control systems are used; they also emulate the dynamic behavior and PFR. The general frequency response with the operating limits corresponding to the Gran Canaria power system are shown in Figure 2. During normal system operation, the frequency is nearly 50 Hz. Notwithstanding, when an event that causes an imbalance between the generation and the demand occurs, the frequency begins to decrease with a slope that depends on the total inertia of the system and the power imbalance, which can be expressed by Equation (31) obtained from the swing equation, Equation (30).

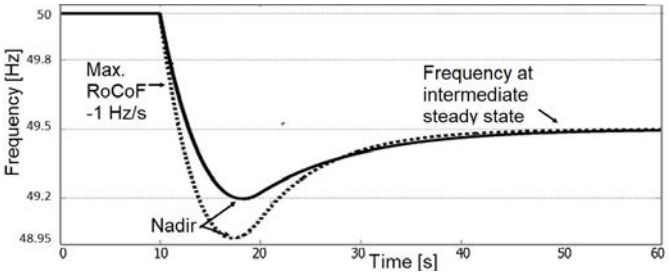

Figure 2. Basic frequency response and limits for the Gran Canaria electrical system.

It is possible to observe the three most singular points in the described curve (characteristic points of a second-order response underdamped): the initial slope (RoCoF), the value of the greatest overshoot (nadir frequency), and the stabilization value (steady state frequency). With respect to the electrical system of Gran Canaria, the limit criterion for the RoCoF is set at -1 Hz/s, and the minimum nadir frequency is set at 48.95 Hz [36]; the basic frequency response corresponding to these limits is represented in Figure 2 by the dotted line. The Canary Islands system operator has developed its own tool to analyze the behavior of the post-contingency frequency [37], which is a simplified dynamic model based on a single node and with the governors modeled as first-order linear systems. In this research, a new tool developed in MATLAB/Simulink [38] has been used to verify the frequency behavior (see Sections 2.2, 4.1, and 4.2), in which the electrical system of Gran Canaria has been modeled as a single node because it is intended to evaluate the evolution of the average system frequency, in other words, the center of inertia (COI). The system model (Figure 3) includes individual models created for each of the conventional thermal generators: two combined cycles, two gas units, and two steam units in Barranco de Tirajana; and two diesel generators, three gas units, and two steam units in Jinamar. In addition, load damping of 1% is included to represent the demand behavior [37]. The PFR of each generator is given by the Equation (31) as follows, where K is the gain of the regulator (the droop inverse value), T_p is the time constant of the primary regulator, $\Delta P_{n,pu}$ is the generator power output change in per unit at a present time n, and the frequency and the power output of the generator at the immediately previous instant are f_{n-1} and P_{n-1}, respectively:

$$\Delta P_{n,pu} = \frac{-(K \cdot f_{n-1} + P_{n-1})}{T_p} \tag{31}$$

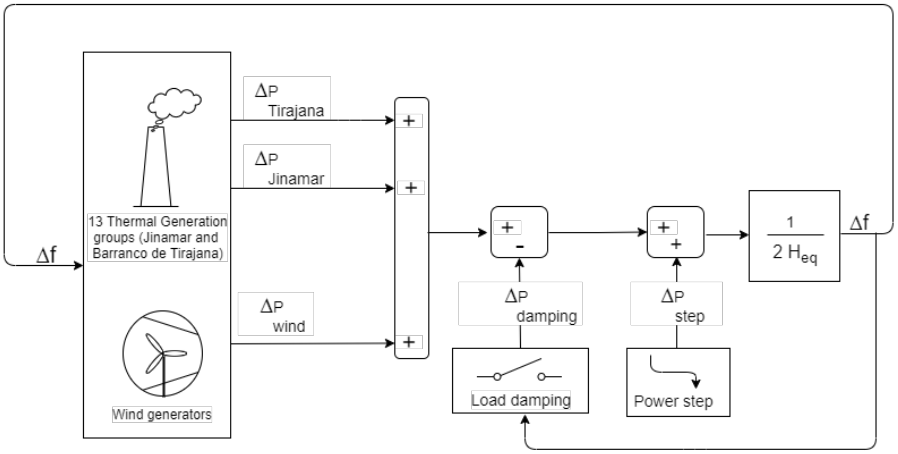

Figure 3. The Gran Canaria power system model.

2.3. UC with Endogenous Frequency Constraints

To account for the new restrictions, the constraint equations described below should be added to the bUC defined by Equations (1)–(8).

2.3.1. Dynamic Reserve Allocation

The fixed predefined reserve constraint could provide an acceptable transient response in large systems. However, although the reserve restriction is met, it could entail a N-1 criterion violation in small systems. Dynamic allocation of the reserve assures the spare system capacity after a contingency is enough to compensate for the power loss from a steady state point of view. The intention is not to over-allocate the spinning reserve to reduce operating costs, but under-dimensioning the spinning reserve incurs a risk for the system's security. This inclusion of a dynamic reserve restriction replaces the static reserve allocation (typically included in the bUC). The following equation describes the dynamic reserve allocation:

$$\sum_{i \neq j}^{I} (p_{it} - p_i^{max}) \geq p_{jt}, t = 1, \ldots, T. \tag{32}$$

2.3.2. Rate of Change of Frequency

The frequency response of an electrical system after a contingency, such as a generator loss, is closely related to the generators' commitment states because they describe the combined system characteristics of droop and inertia.

More specifically, the frequency decay after a generator loss is described by the sum of the survived inertia and the amount of the power loss, as is defined in the following equations. The greatest variation in speed with respect to time occurs at the instant immediately after the contingency t_{0^+}. According to the swing equation, Equation (30),

$$\frac{d}{dt}\Delta f(t) = \frac{1}{M_H}[\Delta P_m(t) - \Delta P_e(t)] \tag{33}$$

Expressing Equation (33) in $t = t_{0^+}$

$$RoCoF = \frac{d}{dt}\Delta f\left(0^+\right) = -\frac{P_l}{M_H} \tag{34}$$

where P_l is the generating unit power suddenly disconnected in watts.

The RoCoF condition is then obtained as follows:

$$M_H \geq \frac{P_l}{|RoCoF_{\max}|} \tag{35}$$

Taking the thermal and wind generators into account, the total system inertia in seconds can be calculated as

$$M_H = \frac{\sum_{i=1}^{N_s} M_{S,i} S_{S,i} + \sum_{i=1}^{N_w} M_{v,i} S_{w,i}}{S_B} \tag{36}$$

where N_s and N_w are the quantity of synchronous and wind generators, respectively; $M_{S,i}$ is the mechanical time constant of the ith synchronous generator, $M_{v,i}$ is the virtual mechanical time constant of the wind turbine; $S_{S,i}$ and $S_{w,i}$ are the i_{th} synchronous generator apparent power and the i_{th} wind turbine apparent power, respectively.

2.3.3. Nadir Frequency

From Equation (30), the constraint of the nadir frequency is derived, integrating Equation (29) as follows:

$$\int_{t_0}^{t_{nadir}} \frac{d}{dt} \Delta f(t) dt = \frac{1}{M_H} \int_{t_0}^{t_{nadir}} (\Delta P_m(t) - \Delta P_e(t)) dt \tag{37}$$

where t_{nadir} is the time when the nadir occurs in seconds.

Applying Equations (12) and (13) in Equation (37) and taking Equation (19) into account yields

$$\Delta f(t_{nadir}) - \Delta f(t_0) = \frac{1}{M_H} \int_{t_0}^{t_{nadir}} (P_m(t) - P_e(t)) dt \tag{38}$$

$$\Delta f(t_{nadir}) = f_{nadir} - f_0 \tag{39}$$

where f_{nadir} is the minimum frequency obtained in Hz.

$$f_{nadir} - f_0 = \frac{1}{M_H} \int_{t_0}^{t_{nadir}} (P_m(t) - P_e(t)) dt \tag{40}$$

After an instantaneous drop in generating power (P_m) of P_l , the simplified (linear) behavior of the primary response is modeled as a slope ramp $c = \frac{\Delta P}{\Delta t}$, which starts after a delay time t_d (due to the dead band frequency). Therefore, the integral is evaluated at two intervals: from t_0 to t_d ($= t_d$) and from t_d to t_{nadir}, as in the following:

$$f_{nadir} - f_0 = \frac{1}{M_H} \int_{t_0}^{t_d} -P_l dt + \frac{1}{M_H} \int_{t_d}^{t_{nadir}} (-P_l + c(t - t_d)) dt \tag{41}$$

$$f_{nadir} - f_0 = -\frac{-P_l t_d}{M_H} + \frac{1}{M_H} \left[-P_l (t_{nadir} - t_d) + \frac{c(t_{nadir} - t_d)^2}{2} \right] \tag{42}$$

For the study intervals, the slope is:

$$c = \frac{P_l}{(t_{nadir} - t_d)} \tag{43}$$

Substituting Equation (42) into Equation (41) yields

$$f_{nadir} - f_0 = -\frac{-P_l t_d}{M_H} + \frac{1}{M_H} \left[-P_l (t_{nadir} - t_d) + \frac{P_l (t_{nadir} - t_d)}{2} \right] \tag{44}$$

Operating on the terms in brackets results in

$$f_{nadir} - f_0 = -\frac{-P_l t_d}{M_H} + \frac{1}{M_H} \left[-\frac{P_l (t_{nadir} - t_d)}{2} \right] \tag{45}$$

$$f_{nadir} - f_0 = -\frac{-P_l t_d}{M_H} + \frac{1}{M_H} \left[-\frac{P_l^2}{2c} \right] = -\frac{1}{M_H} \left[P_l t_d + \frac{P_l^2}{2c} \right] \tag{46}$$

$$P_l t_d + \frac{P_l^2}{2c} \leq M_H(f_{\min} - f_0) \tag{47}$$

$$\frac{P_l^2}{2c} \leq M_H(f_{\min} - f_0) - P_l t_d \tag{48}$$

Doing the inverse of the above inequality, the following can be obtained:

$$\frac{2c}{P_l^2} = \frac{1}{M_H(f_{\min} - f_0) - P_l t_d} \tag{49}$$

The ramp c would then be

$$c \geq \frac{\frac{1}{2}P_l^2}{M_H(f_{\min} - f_0) - P_l t_d} \tag{50}$$

Immediately after the contingency, in the first interval (up to t_d), the behavior of the system is inertial, and the frequency variation only depends on the contingency (P_l) and the system inertia (M_H). Therefore,

$$t_d = f_{db}\frac{M_H}{P_l} \tag{51}$$

Substituting Equation (51) into Equation (50) results in

$$c \geq \frac{\frac{1}{2}P_l^2}{M_H(f_{\min} - f_0 - f_{db})} \tag{52}$$

As for $c_{\min}$, the response ramp of the system with which $f_{\min}$ would be obtained, it can be calculated as

$$c_{\min} = \frac{P_l^2}{2M_H(f_{\min} - f_0 - f_{db})} \tag{53}$$

In addition, the response power delivered by a generator (p_i^{nadir}) would be its ramp (c_i) times the response time, that is, the time since the regulator action starts (t_d) until the power balance is restored (t_{nadir}), as in the following:

$$p_i^{nadir} = c_i(t_{nadir} - t_d) \tag{54}$$

where c_i is the ramp capacity or the maximum power ramp of generator i.

The generator i will not deliver more power than that it is capable in the time interval (depending on its ramp); therefore, the generator's provided reserve r_i would be, at most, this response power (p_i^{nadir}).

$$r_i \leq c_i(t_{nadir} - t_d) \tag{55}$$

In other words, it cannot be assigned a primary response power greater than that which it is capable of giving in the primary response time. Meeting this restriction prevents the frequency from dropping below the minimum, ensuring the generator will deliver its reserve allocation within the response interval. If it is assigned $r_i \leq p_i^{nadir}$, it will be able to deliver that amount on time. If $r_i \geq p_i^{nadir}$, then the reserve allocation will be limited by the generator (r_i) to force compliance with the constraint Equation (55), and the new allocated reserve will then be able to be delivered on time.

Substituting Equation (42) into Equation (55):

$$r_i \leq c_i\frac{P_l}{c_{\min}} \tag{56}$$

Including $c_{\min}$ implies taking into account the worst case because the lower the ramp c, the lower the nadir frequency. Substituting Equation (53) into Equation (56) yields

$$r_i \leq c_i\frac{2M_H(f_{\min} - f_0 - f_{db})}{P_l} \tag{57}$$

3. Electrical Generation System of Island of Gran Canaria

Table 2 shows the main power characteristics and the date of registration of the thermal generators in Gran Canaria [39]. Although the electrical system of Gran Canaria has 16 generation groups in two conventional thermal power plants, Jinámar and Barranco de Tirajana, only 13 groups are in operation since the oldest diesel generators at the Jinámar power plant have not been programmed to operate for at least eight years [40]. In addition, the combined cycles are not programmed at the mode in which they are capable of delivering their maximum power (gas and gas and steam) above 200 MW; rather, in practice, they only operate in the gas and steam mode, reaching a maximum power of 103.05 MW and 113.5 MW for Combined Cycles 1 and 2, respectively. Therefore, 13 thermal generation groups have been considered, resulting in a combined conventional capacity of 664 MW.

Table 2. Gran Canaria generation units.

Register Number	Power Plant Name	Max Power MW	Min Power MW	Discharge Date
RO2-0089	BARRANCO DE TIRAJANA 1. GAS 1	32.34	6.79	01/07/1992
RO2-0090	BARRANCO DE TIRAJANA 2, GAS 2	32.34	6.79	11/05/1995
RO1-1049	BARRANCO DE TIRAJANA 3, VAPOR 1	74.24	27.84	01/01/1996
RO1-1050	BARRANCO DE TIRAJANA 4, VAPOR 2	74.24	27.84	05/06/1996
RO1-1051		68.7	9.70	19/07/2003
RO1-1052	BARRANCO DE TIRAJANA, CC1	103.05	37.80	21/08/2003
RO1-2000		206,1	75.50	22/11/2004
RO2-0188		75.0	9.70	01/08/2006
RO2-0189	BARRANCO DE TIRAJANA. CC2	113.5	37.80	27/11/2006
RO2-0190		227.0	75.50	18/06/2008
RO2-0087	JINAMAR 10. GAS 2	32.34	6.79	26/01/1989
RO2-0088	JINAMAR 11, GAS 3	32.34	6.79	01/05/1989
RO2-0084	JINAMAR 12, DIESEL 4	20.51	14.09	07/06/1990
RO2-0085	JINAMAR 13, DIESEL 5	20.51	14.09	08/08/1990
RO2-0081	JINAMAR 2, DIESEL 1	8.51	4.58	01/02/1973
RO2-0082	JINAMAR 3, DIESEL 2	8.51	4.58	27/08/1973
RO2-0083	JINAMAR 4, DIESEL 3	8.51	4.58	01/02/1974
RO2-0086	JINAMAR 7, GAS 1	17.64	6.79	21/04/1981
RO1-1047	JINAMAR 8, VAPOR 4	55.56	17.7	01/08/1982
RO1-1048	JINAMAR 9, VAPOR 5	55.56	17.7	05/12/1984

The electrical system of Gran Canaria has experienced two major blackouts related to the disconnection of generators on 9 August 2011 and 5 December 2012, resulting in a power outage of practically the entire island (during the first) and half of the territory of Gran Canaria (during the second). In Gran Canaria islands, the values of energy not supplied and the average time of interruption of the supply in 2019 were 41 times higher than the values registered in 2018 [41].

On 16 September 2020, there was a failure again, leaving several neighborhoods of the city of Las Palmas de Gran Canaria without electricity. Furthermore, the nearby island of Tenerife, with similar characteristics, suffered total blackouts caused by failures in generating plants in September 2019 and in July 2020. The increase in renewable technologies can even increase the incidence of these events by reducing the system inertia and its PFR, thus increasing the variability. If there are no elements able to compensate for this variation, the security of the system could be at risk.

4. Results

For this examination, five critical cases were selected from among those that have occurred on Gran Canaria in the last nine years. The three simulation tools developed for this analysis were then applied to the selected cases: the bUC, the dynamic frequency

checking, and the FCUC tool. Finally, the UC results are presented for both the bUC (Section 4.1) and the FCUC tool (Section 4.2). In all the scenarios and simulated hours, the RoCoF and nadir frequency values reached were analyzed based on the restrictions included in each UC tool. The frequency results were contrasted, and the costs associated with each tool were compared.

For this article, five 24-h scenarios have been simulated corresponding to the real demand of Gran Canaria island on 05/12/2012, 03/06/2018, 28/10/2018, 01/11/2018, and 08/11/2020, which are referred to as Cases 1 to 5, respectively (Table 3). These scenarios were selected either because of a major blackout that occurred that day or the greatest load fraction was committed to the combined cycle plant, thus representing a risk for system stability in the case of a contingency at that plant. The simulated cases had demands that varied between 238 MW (in hour 3 of Case 3) to 509 MW (in hour 21 of Case 1). The average renewable penetration percentages varied from 1.5% in Case 1 to 29.3% in Case 2 (Table 3). The most relevant case in terms of the renewable fraction is Case 2, where the renewable percentage ranges from 22% to 37% in hours 21 and 17, respectively (Figure 4).

These scenarios have been simulated in the three tools developed by the authors for this study: the bUC software tool (in Python, see Section 4.1), the dynamic frequency checking tool (in MATLAB/Simulink, see Sections 2.2, 4.1, and 4.2), and the UC software tool with dynamic reserve and RoCoF constraints (in Python, see Section 4.2). The commitment tool used by the Gran Canaria system operator has been used with the purpose of validating the bUC tool created ad hoc in the Python programming language.

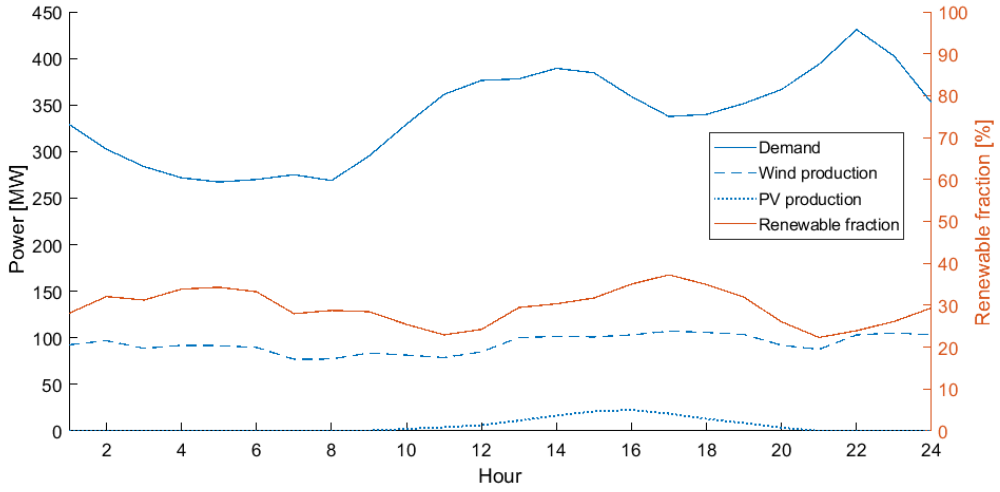

Figure 4. Case 2 demand, wind and PV production, and renewable fraction.

The technical data of the generators related to their power limits and start-up, operating, and maintenance costs have been obtained from [39]. Other parameters related to operating restrictions have been provided by the transmission system operator's [37] tools.

Table 3. Hourly demand (MW) and average renewable penetration (%) for five cases.

Case	**1**	**2**	**3**	**4**	**5**
Hour					
1	325.80	329.33	335.27	334.13	312.05
2	293.33	302.50	311.37	312.03	290.53
3	274.63	283.83	237.63	300.83	275.50
4	267.90	271.83	277.53	292.08	265.72
5	267.33	267.33	275.70	290.30	262.18
6	276.87	270.00	278.67	289.65	263.52
7	321.23	275.17	287.05	302.08	273.47
8	385.32	268.83	291.33	304.95	271.42
9	417.63	295.22	328.70	342.82	298.85
10	285.50	329.40	366.63	380.70	337.18
11	378.08	361.37	392.20	402.72	361.50
12	432.93	376.40	402.40	407.45	376.23
13	446.63	378.08	414.23	412.28	385.38
14	464.97	389.30	426.08	421.27	399.55
15	463.43	384.53	412.50	415.00	392.05
16	448.93	358.97	378.92	387.93	362.58
17	435.83	337.63	360.55	367.62	348.45
18	436.47	339.93	367.82	374.73	352.70
19	481.13	351.68	397.67	406.20	386.88
20	508.68	366.65	439.53	438.83	416.37
21	509.23	393.70	445.08	440.67	421.43
22	492.87	431.00	420.38	421.67	398.58
23	435.08	402.50	372.43	379.83	360.23
24	382.90	352.50	332.50	339.88	322.47
Renewable Penetration (%)	1.5%	29.3%	10.2%	10.7%	6.5%

4.1. Basic Unit Commitment

The generators scheduling solution obtained in the Python bUC tool (with exogenous frequency constraints) for the five 24-h scenarios has been subsequently evaluated by the MATLAB/Simulink dynamic tool. The nadir frequency and RoCoF results are shown in Figures 5 and 6.

Although the frequency thresholds that activate the disconnection to protect the generator turbine were 47.5 Hz and −2 Hz/s [1], the limits that activate the load shedding are more strict. In any case, it is generally recommended [42] that the absolute value of the frequency for load shedding should not be less than 49 Hz, while in NORDEL and Ireland ESB, the load shedding frequency was 48.8 Hz and 48.5 Hz, respectively. In regard to the activation of load shedding by the derivative of the frequency, −0.5 Hz/s was proposed in [6] for the system on Gran Canaria island. Nevertheless, a specific load shedding plan exists for each island [43]. Regarding the Gran Canaria power system, the admissibility criterion set the limit for both the RoCoF and nadir frequency at −1 Hz/s and 48.95 Hz, respectively [36].

When the bUC was simulated in the case of contingency, the worst post-contingency RoCoF values went from −1.34 Hz/s in Case 1 (hour 1) up to −1.43 Hz/s in Case 2 (hour 22), as shown in Figures 5 and 6, according to the scenario with the highest proportion of renewables and the time when there was a greater increase in demand.

Furthermore, the worst nadir fall values ranged from 48.61 Hz in Case 1 (hour 1) up to 48.47 Hz in Case 2 (hour 24), representing a risk to the system. In all cases, there were some hours within which the RoCoF exceeded −1 Hz/s, and the nadir frequency fell below 49.85 Hz (Figures 5 and 6).

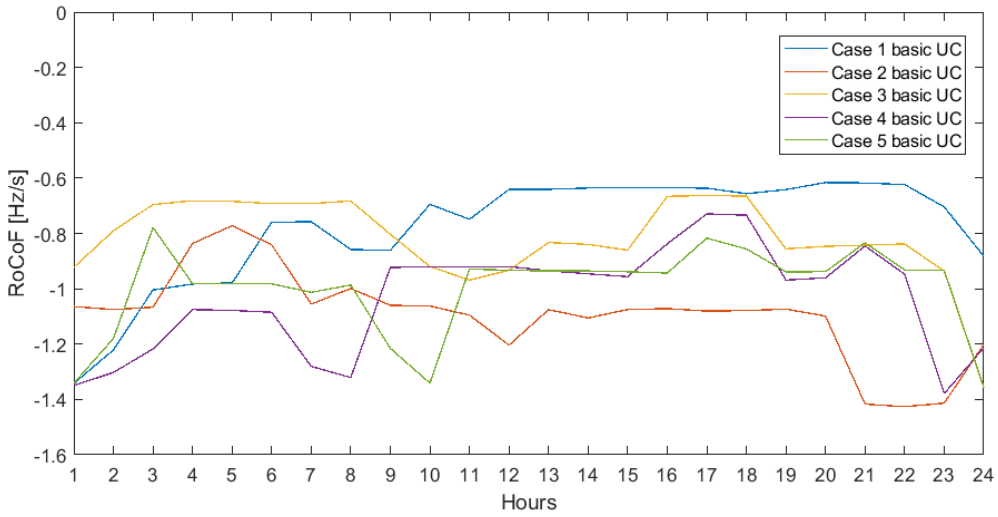

Figure 5. 24-h RoCoF for five cases applying bUC.

Therefore, in terms of increasing system reliability, it would be recommended to modify the commitment results after the subsequent risk checkup.

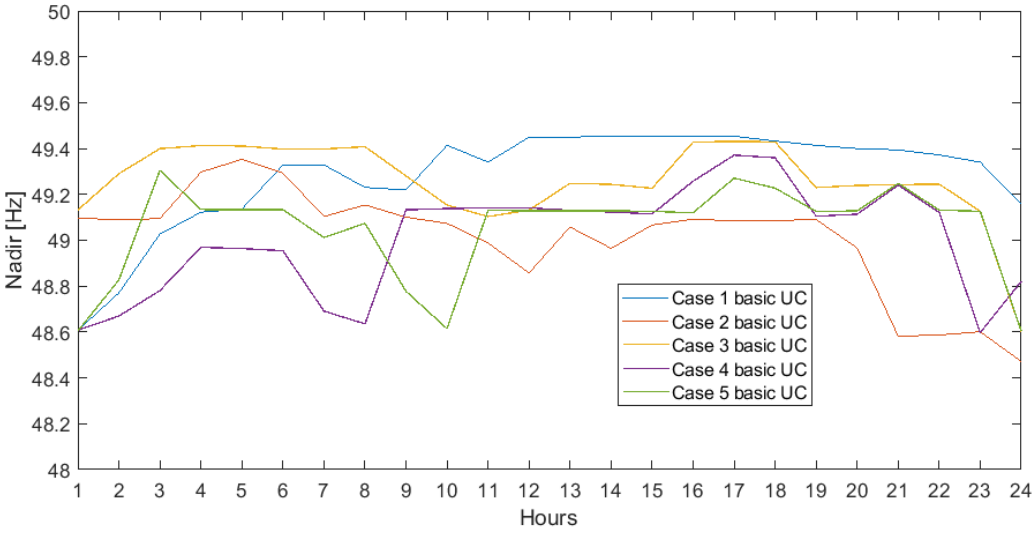

Figure 6. 24-h nadir for five cases of basic UC.

4.2. Frequency-Constrained Unit Commitment

In this section, the same scenarios as in Section 4.1 have been simulated, but we incorporated new constraints to the bUC to ensure that the gradient of the frequency drop as well as the nadir fall, in case of a serious contingency N-1, are reduced. The idea behind the two constraints is to provide enough inertia to limit the initial frequency fall and to ensure that the available headroom in "survivor" generators at any time is enough to cover the maximum power committed to a generator.

Regarding the arrest of a post-contingency frequency fall, two constraints have been considered: the first is applied on the dynamic reserve allocation, and the second is applied on the RoCoF. Both post-contingency frequency measurements, nadir and RoCoF, are enhanced by including either one constraint, the other, or both. In Figures 7 and 8, the results of the FCUC for Case 2 (the case with the largest renewable fraction) with the incorporation of the RoCoF and dynamic reserve constraints to the bUC problem are shown.

With the dynamic reserve constraint, the greatest improvements occurred in Case 4 at hour 2, where the RoCoF was reduced by 54.13% and the nadir fall was reduced by 61.38%.

For both the RoCoF constraint and the combination of the dynamic reserve plus RoCoF constraints, the greatest improvements occurred in Case 5 at hour 10, where the RoCoF was reduced by 64.77% and the nadir reduced by 71.33% (Figure 9). In all cases, including the RoCoF constraint in any way, there was no hour within which the RoCoF exceeded −1 Hz/s, and the nadir fell below 49.85 Hz (Figures 10 and 11, Table 4).

Note that the improvements showed up whether both constraints were included or if only the RoCoF constraint was included, so it can be seen that the RoCoF constraint was more restrictive than that of the dynamic reserve (Table 4).

The cost results split into all considered cost types, i.e., start-up, regulation, operational, and O&M costs, are shown in Table 5. It can be noted that in all cases the bUC yields the least beneficial cost solution since the inclusion of additional constraints increases the total system operation costs.

Therefore, the commitment results improved the system security in terms of frequency stability in case of a contingency, with the drawback of increasing the operating costs of the system from 2.7% in Case 1 when incorporating the dynamic reserve constraint and up to 12.8% in Case 2 when incorporating both the dynamic reserve and RoCoF constraints (Tables 4 and 6).

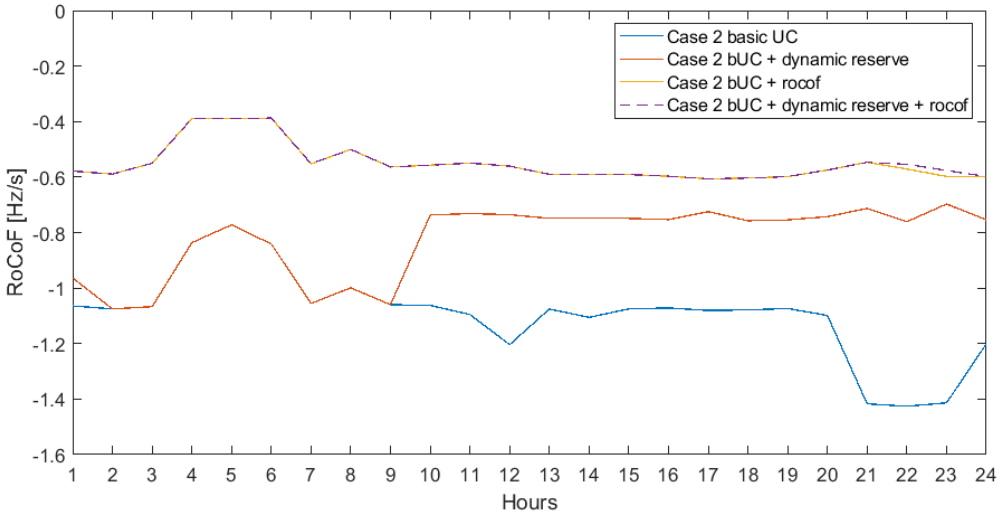

Figure 7. 24-h Case 2 RoCoF under various constraints.

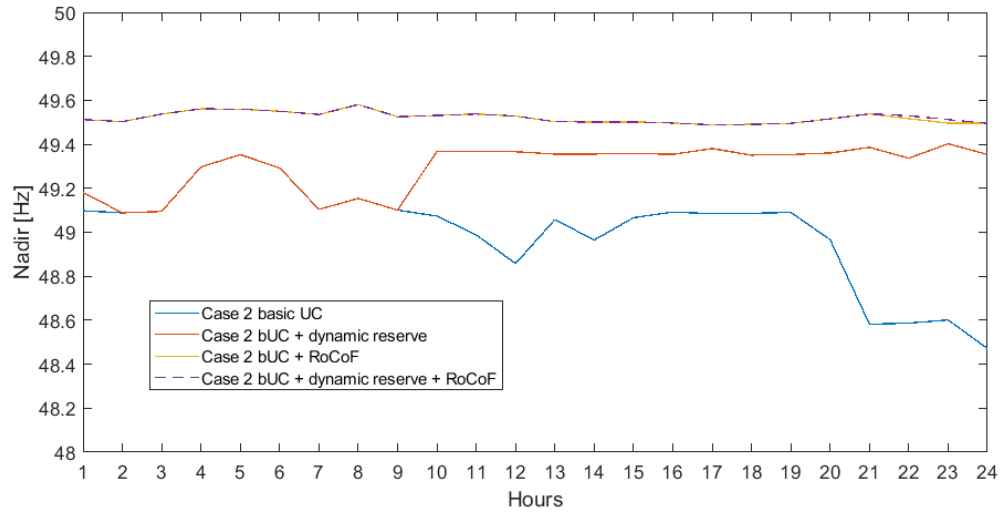

Figure 8. 24-h Case 2 nadir under various constraints.

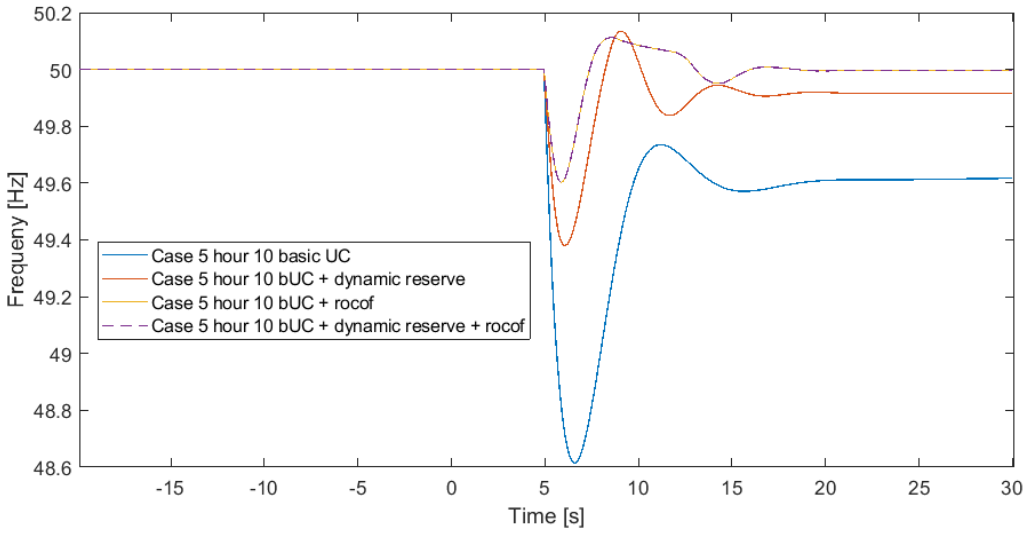

Figure 9. Case 5 at hour 10, post-contingency frequency behavior.

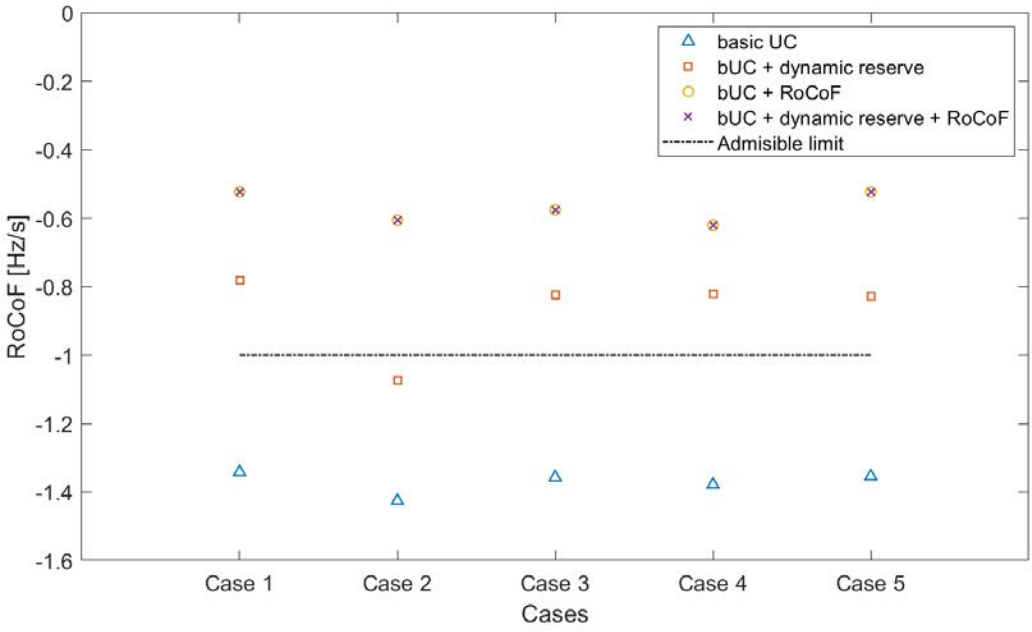

Figure 10. Worst RoCoF obtained with each constraint in the five cases.

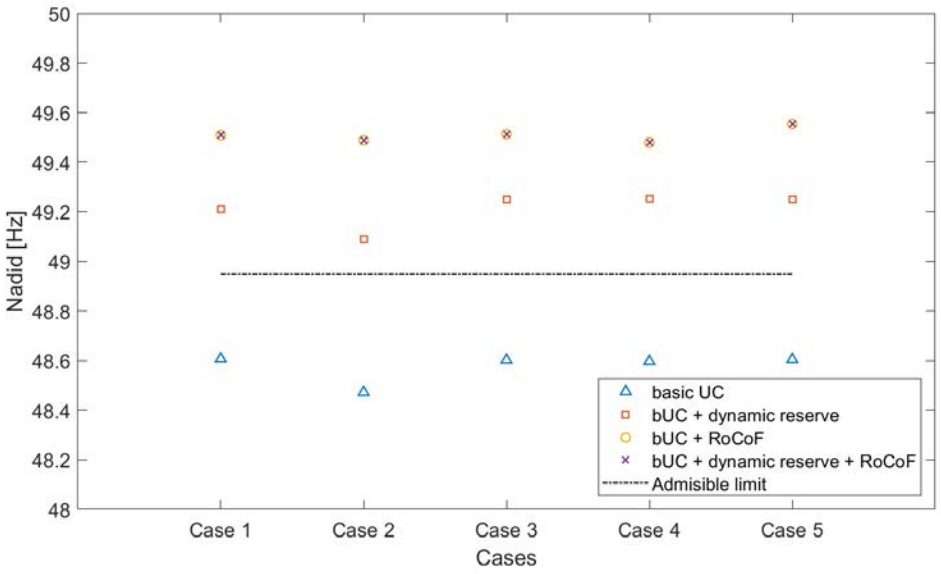

Figure 11. Worst nadir obtained with each constraint in the five cases.

Table 4. Minimum RoCoF and Nadir for the five cases and the three ways of constraint use.

Case Number	**Constraints Used**			
Case 1	bUC	dynamic reserve	RoCoF	dynamic reserve + RoCoF
Mín RoCoF (Hz/s)	−1.34	−0.78	−0.52	−0.52
Mín Nadir (Hz)	48.61	49.21	49.51	49.51
Case 2	bUC	dynamic reserve	RoCoF	dynamic reserve + RoCoF
Mín RoCoF (Hz/s)	−1.43	−1.08	−0.61	−0.61
Mín Nadir (Hz)	48.47	49.09	49.49	49.49
Case 3	bUC	dynamic reserve	RoCoF	dynamic reserve + RoCoF
Mín RoCoF (Hz/s)	−1.36	−0.82	−0.58	−0.58
Mín Nadir (Hz)	48.60	49.25	49.51	49.51
Case 4	bUC	dynamic reserve	RoCoF	dynamic reserve + RoCoF
Mín RoCoF (Hz/s)	−1.38	−0.82	−0.62	−0.62
Mín Nadir (Hz)	48.60	49.25	49.48	49.48
Case 5	bUC	dynamic reserve	RoCoF	dynamic reserve + RoCoF
Mín RoCoF (Hz/s)	−1.35	−0.83	−0.52	−0.52
Mín Nadir (Hz)	48.60	49.25	49.55	49.55

Table 5. Total operational cost breakdown for the five cases and the three ways of constraint use.

Case Number and Cost Breakdown	**Constraints Used**			
Case 1	bUC	dynamic reserve	RoCoF	dynamic reserve + RoCoF
Start-Up Cost (EUR)	82,739	91,506	91,506	91,506
Regulation Cost (EUR)	7926	8078	8322	8322
Operational Cost (EUR)	792,625	807,780	832,158	832,158
O&M Cost (EUR)	212	212	207	207
Total Operation Cost (EUR)	883,502	907,576	932,192	932,192
Case 2	bUC	dynamic reserve	RoCoF	dynamic reserve + RoCoF
Start-Up Cost (EUR)	0	33,397	24,629	29,013
Regulation Cost (EUR)	4461	4539	4744	4747
Operational Cost (EUR)	446,056	453,857	474,372	474,627
O&M Cost (EUR)	136	134	133	134
Total Operation Cost (EUR)	450,652	491,926	503,879	508,519
Case 3	bUC	dynamic reserve	RoCoF	dynamic reserve + RoCoF
Start-Up Cost (EUR)	24,629	42,164	78,355	78,355
Regulation Cost (EUR)	6372	6594	6410	6410
Operational Cost (EUR)	637,162	659,372	641,047	641,047
O&M Cost (EUR)	173	172	177	177
Total Operation Cost (EUR)	668,336	708,302	725,990	725,990
Case 4	bUC	dynamic reserve	RoCoF	dynamic reserve + RoCoF
Start-Up Cost (EUR)	24,629	42,164	73,972	73,972
Regulation Cost (EUR)	6432	6682	6519	6519
Operational Cost (EUR)	643,193	668,192	651,928	651,928
O&M Cost (EUR)	178	176	180	180
Total Operation Cost (EUR)	674,432	717,214	732,599	732,599
Case 5	bUC	dynamic reserve	RoCoF	dynamic reserve + RoCoF
Start-Up Cost (EUR)	24,629	37,780	78,355	29,013
Regulation Cost (EUR)	6209	6476	6340	4746
Operational Cost (EUR)	620,934	647,570	634,025	474,627
O&M Cost (EUR)	174	171	176	134
Total Operation Cost (EUR)	651,946	691,997	718,897	718,897

Table 6. Operational cost increase in percentage for the five cases and the three ways of constraint use.

Operational Cost Increase in Percentage					
Constraint	Case 1	Case 2	Case 3	Case 4	Case 5
Dynamic reserve	2.72%	9.16%	5.98%	6.34%	6.14%
RoCoF	5.51%	11.81%	8.63%	8.62%	10.27%
Dynamic reserve + RoCoF	5.51%	12.84%	8.63%	8.62%	10.27%

5. Discussion and Conclusions

The electrical system of Gran Canaria island has suffered several episodes of greater blackouts in recent years. The UC by itself, although it will provide the most economical solution, is not capable of ensuring the safe operation of the microgrid after a contingency, as the system frequency may fall under the activation of UFLS limits. The authors have developed three tools to: (1) emulate the UC currently applied by the island's electrical operator (bUC), (2) simulate its dynamics, and (3) incorporate the restrictions that prevent the frequency limits from being exceeded into in the UC (FCUC). Critical scenarios have been selected: five cases in which protections had been breached in the last nine years. When the bUC tool was evaluated, as expected in all cases, both the RoCoF and the nadir frequency went beyond the limits because critical cases had been selected. The bUC showed that the limits were reached earlier in situations with a higher rate of penetration

of renewables. The new FCUC, including both the RoCoF and dynamic reserve constraints, avoided reaching the frequency limits in the five simulated scenarios; according to the obtained results, the most restrictive constraint is the RoCoF. There has been a maximum reduction of 65% in the value of the RoCoF and a maximum reduction of 71% in the value of the nadir frequency. In contrast, to obtain those improvements in the scenario of higher renewable penetration, the system operational costs increased around 13%. The increase in the system's operational cost could be taken into account to estimate how to remunerate the safety service based on the value of the additional reserve provision to the system.

Author Contributions: Conceptualization, D.R., M.C. and D.S.-M.; methodology, D.R. and D.S.-M.; software, D.R.; validation, D.R.; formal analysis, D.R., M.C. and J.M.G.; investigation, D.R. and M.C.; resources, D.S.-M. and J.M.G.; data curation, D.S.-M. and J.M.G.; writing—original draft preparation, D.R. and M.C.; writing—review and editing, M.C. and D.S.-M.; visualization, D.S.-M.; supervision, D.S.-M. and J.M.G.; project administration, D.R., M.C. and D.S.-M. All authors have read and agreed to the published version of the manuscript.

Funding: 1-This work was supported by the Spanish Ministry of Innovation under Grant PID2019-104449RB-I00. 2-This work was supported by VILLUM FONDEN under the VILLUM Investigator Grant (no. 25920): Center for Research on Microgrids (CROM); www.crom.et.aau.dk, accessed on 1 May 2021.

Institutional Review Board Statement: Not applicable.

Informed Consent Statement: Not applicable.

Data Availability Statement: Excluded due to company's confidential data.

Acknowledgments: This work was supported by VILLUM FONDEN under the VILLUM Investigator Grant (no. 25920): Center for Research on Microgrids (CROM); www.crom.et.aau.dk, accessed on 1 May 2021.

Conflicts of Interest: The authors declare no conflict of interest.

References

1. Ministerio de Energía, Turismo y Agenda Digital, España, Resolución de 1 de febrero de 2018 de la Secretaría de Estado de Energía por la que se aprueba el procedimiento de operación 12.2 "Instalaciones conectadas a la red de transporte y equipo generador: Requisitos mínimos de diseño, equipamiento, funcionamiento, puesta en servicio y seguridad" de los sistemas eléctricos no peninsulares, 2018. Available online: https://www.boe.es/boe/dias/2018/02/16/pdfs/BOE-A-2018-2198.pdf (accessed on 1 November 2019).
2. Daly, P.; Flynn, D.; Cunniffe, N. Inertia considerations within unit commitment and economic dispatch for systems with high non-synchronous penetrations. In Proceedings of the 2015 IEEE Eindhoven PowerTech, Eindhoven, The Netherlands, 29 June–2 July 2015; pp. 1–6.
3. Kundur, P. *Power System Stability and Control*; McGraw-Hill: New York, NY, USA, 1994.
4. Lokay, H.E.; Burtnyk, V. Application of Underfrequency Relays for Automatic Load Shedding. *IEEE Trans. Power Appar. Syst.* **1968**, *PAS-87*, 776–783. [CrossRef]
5. Xie, L.; Carvalho, P.M.S.; Ferreira, L.A.F.M.; Liu, J.; Krogh, B.H.; Popli, N.; Ilić, M.D. Wind Integration in Power Systems: Operational Challenges and Possible Solutions. *Proc. IEEE* **2011**, *99*, 214–232. [CrossRef]
6. Sigrist, L.; Lobato, E.; Echavarren, F.; Egido, I.; Rouco, L. *Island Power Systems*; CRC Press Taylor & Francis Group: Boca Raton, FL, USA, 2016.
7. Jayawardena, A.V.; Meegahapola, L.G.; Perera, S.; Robinson, D.A. Dynamic characteristics of a hybrid microgrid with inverter and non- inverter interfaced renewable energy sources: A case study. In Proceedings of the 2012 IEEE International Conference on Power System Technology (POWERCON), Auckland, New Zealand, 23–26 October 2012; pp. 1–6.
8. Restrepo, J.F.; Galiana, F.D. Unit commitment with primary frequency regulation constraints. *IEEE Trans. Power Syst.* **2005**, *20*, 1836–1842. [CrossRef]
9. Chang, G.W.; Chuang, C.; Lu, T.; Wu, C. Frequency-regulating reserve constrained unit commitment for an isolated power system. *IEEE Trans. Power Syst.* **2013**, *28*, 578–586. [CrossRef]
10. Kërçi, T.; Milano, F. A Framework to embed the Unit Commitment Problem into Time Domain Simulations. In Proceedings of the 2019 IEEE International Conference on Environment and Electrical Engineering and 2019 IEEE Industrial and Commercial Power Systems Europe (EEEIC/I CPS Europe), Genova, Italy, 10–14 June 2019; pp. 1–5.
11. Wu, Z.; Gao, W.; Gao, T.; Yan, W.; Zhang, H.; Yan, S.; Wang, X. State-of-the-art review on frequency response of wind power plants in power systems. *J. Mod. Power Syst. Clean Energy* **2018**, *6*, 1–16. [CrossRef]

12. Cardozo, C.; Capely, L.; Dessante, P. Frequency constrained unit commitment. *Energy Syst.* **2017**, *8*, 31–56. [CrossRef]
13. Fei Teng.; Trovato, V.; Strbac, G. Stochastic scheduling with inertia-dependent fast frequency response requirements. In Proceedings of the 2016 IEEE Power and Energy Society General Meeting (PESGM), Boston, MA, USA, 17–21 July 2016; p. 1. [CrossRef]
14. Cardozo Arteaga, C. Optimisation of Power System Security with High Share of Variable Renewables: Consideration of the Primary Reserve Deployment Dynamics on a Frequency Constrained Unit Commitment Model. Ph.D. Thesis, Université Paris-Saclay (ComUE), Paris, France, 2016.
15. Doherty, R.; Lalor, G.; O'Malley, M. Frequency control in competitive electricity market dispatch. *IEEE Trans. Power Syst.* **2005**, *20*, 1588–1596. [CrossRef]
16. Cardozo, C.; Capely, L.; van Ackooij, W. Cutting plane approaches for the frequency constrained economic dispatch problems. *Electr. Power Syst. Res.* **2018**, *156*, 54–63. [CrossRef]
17. Rabbanifar, P.; Amjady, N. Frequency-constrained unit-commitment using analytical solutions for system frequency responses considering generator contingencies. *IET Gener. Transm. Distrib.* **2020**, *14*, 3548–3560. [CrossRef]
18. Lemaréchal, C.; Renaud, A. A geometric study of duality gaps, with applications. *Math. Program.* **2001**, *90*, 399–427. [CrossRef]
19. van Ackooij, W. Large-scale unit commitment under uncertainty: An updated literature survey. *Ann. Oper. Res. Univ. Pisa* **2018**, *271*, 11–85. [CrossRef]
20. Ummels, B.C.; Gibescu, M.; Pelgrum, E.; Kling, W.L.; Brand, A.J. Impacts of Wind Power on Thermal Generation Unit Commitment and Dispatch. *IEEE Trans. Energy Convers.* **2007**, *22*, 44–51. [CrossRef]
21. Tuohy, A.; Denny, E.; Meibom, P.; Barth, R.; O'Malley, M. Operating the Irish power system with increased levels of wind power. In Proceedings of the 2008 IEEE Power and Energy Society General Meeting—Conversion and Delivery of Electrical Energy in the 21st Century, Pittsburgh, PA, USA, 20–24 July 2008; pp. 1–4.
22. Zhang, Z.; Du, E.; Teng, F.; Zhang, N.; Kang, C. Modeling Frequency Dynamics in Unit Commitment With a High Share of Renewable Energy. *IEEE Trans. Power Syst.* **2020**, *35*, 4383–4395. [CrossRef]
23. Melhorn, A.C.; Mingsong Li.; Carroll, P.; Flynn, D. Validating unit commitment models: A case for benchmark test systems. In Proceedings of the 2016 IEEE Power and Energy Society General Meeting (PESGM), Boston, MA, USA, 17–21 July 2016; pp. 1–5. [CrossRef]
24. Denis Lee Hau Aik. A general-order system frequency response model incorporating load shedding: Analytic modeling and applications. *IEEE Trans. Power Syst.* **2006**, *21*, 709–717. [CrossRef]
25. Ela, E.; O'Malley, M. Studying the Variability and Uncertainty Impacts of Variable Generation at Multiple Timescales. *IEEE Trans. Power Syst.* **2012**, *27*, 1324–1333. [CrossRef]
26. Ahmadi, H.; Martí, J.R.; Moshref, A. Piecewise linear approximation of generators cost functions using max-affine functions. In Proceedings of the 2013 IEEE Power Energy Society General Meeting, Vancouver, BC, Canada, 21–25 July 2013; pp. 1–5. [CrossRef]
27. Ahmadi, H.; Ghasemi, H. Security-Constrained Unit Commitment With Linearized System Frequency Limit Constraints. *IEEE Trans. Power Syst.* **2014**, *29*, 1536–1545. [CrossRef]
28. Riaz, S.; Verbič, G.; Chapman, A.C. Computationally Efficient Market Simulation Tool for Future Grid Scenario Analysis. *IEEE Trans. Smart Grid* **2019**, *10*, 1405–1416. [CrossRef]
29. Ministerio para la Transición Ecológica y el Reto Demográfico, España, (EOLCAN) Ayudas a la Inversión en Instalaciones de Producción de Energía Eléctrica de Tecnología Eólica Situadas en Canarias. 2020. Available online: https://sede.idae.gob.es/lang/extras/tramites-servicios/2020/EOLCAN_2/Resolucion_IDAE_convocatoria_EOLCAN_2.pdf (accessed on 1 April 2021).
30. Ministerio para la Transición Ecológica y el Reto Demográfico, España, (SOLCAN) Programa de Ayudas a la Inversión en Instalaciones de Producción de Energía Eléctrica de Tecnología Solar Fotovoltaica Situadas en Canarias Cofinanciadas con Fondos Comunitarios FEDER. 2020. Available online: https://sede.idae.gob.es/lang/extras/tramites-servicios/2020/SOLCAN/Resolucion_convocatoria_Solcan_de_24_de_junio_de_2020.pdf (accessed on 1 April 2021).
31. Ministerio para la Transición Ecológica y el Reto Demográfico, España, Investment Aid Programme for Electrical Energygeneration Installations with Wind Power Technology Located in Canarias, Co-Financed with Community Funds from the Erdf. 2021. Available online: https://www.pap.hacienda.gob.es/bdnstrans/GE/es/convocatoria/633341/document/254913 (accessed on 1 March 2021).
32. Tseng, C.L. On Power System Generation unit Commitment Problems. Ph.D. Thesis, University of California, Berkeley, CA, USA, 1996.
33. Paturet, M. Economic Valuation and Pricing of Inertia in Inverter-Dominated Power Systems. Master's Thesis, Swiss Federal Institute of Technology, (ETH), Zurich, Switzerland, 2019. Available online: https://arxiv.org/abs/2005.11029 (accessed on 1 March 2021).
34. Badesa, L.; Teng, F.; Strbac, G. Pricing inertia and Frequency Response with diverse dynamics in a Mixed-Integer Second-Order Cone Programming formulation. *Appl. Energy* **2020**, *260*, 114334. [CrossRef]
35. Richard, T.; Byerly, E.W.K. *Stability of Large Electric Power Systems*; IEEE Press: New York, USA, 1974.
36. Estudios de Prospectiva del Sistema y Necesidades para su Operabilidad, Red Eléctrica de España. 2020. Available online: https://www.ree.es/sites/default/files/01_ACTIVIDADES/Documentos/Prospectiva_y_Operabilidad_Reunion_GSP29Sep20.pdf (accessed on 1 May 2021).

37. Rodríguez-Bobada, F.; Izquierdo, C.; Soto, J.; Cuevas, R.; Santos, P.; Corujo, R. Simplified Frequency Stability Tool for Isolated Systems: ADin. In Proceedings of the 3rd International Hybrid Power Systems Workshop, Tenerife, Spain, 8–9 May 2018.
38. MATLAB. *Version R2020b*; The MathWorks Inc.: Natick, MA, USA, 2020.
39. Ministerio de Industria, Energía Y Turismo, España, Real Decreto 738/2015 de 31 de Julio por el que se Regula la Actividad de Producción de Energía Eléctrica y el Procedimiento de Despacho en los Sistemas Eléctricos de los Territorios no Peninsulares. 2015. Available online: https://www.boe.es/boe/dias/2015/08/01/pdfs/BOE-A-2015-8646.pdf (accessed on 1 May 2021).
40. REE Web Repository of Historical Hourly Generation Data. 2021. Available online: https://demanda.ree.es/visiona/canarias/gcanaria/ (accessed on 1 May 2021).
41. El sistema eléctrico español,2019, Departamento de Acceso a la Información del Sistema Eléctrico de REE, Red Eléctrica de España. 2020. Available online: https://www.ree.es/sites/default/files/11_PUBLICACIONES/Documentos/InformesSistemaElectrico/2019/inf_sis_elec_ree_2019.pdf (accessed on 1 May 2021).
42. ENTSO-E Network Code for Requirements for Grid Connection Applicable to all Generators, European Network of Transmission System Operators (ENTSO-E). 2013. Available online: https://eepublicdownloads.entsoe.eu/clean-documents/pre2015/resources/RfG/130308_Final_Version_NC_RfG.pdf (accessed on 1 May 2021).
43. Criterios Generales de Protección de los Sistemas Eléctricos Insulares y eXtrapeninsulares, Red Eléctrica de España. 2005. Available online: https://www.ree.es/sites/default/files/downloadable/criterios_proteccion_sistema_2005_v2.pdf (accessed on 1 May 2021).